

Electrical and structural properties of antimony-doped p-type ZnO nanorods with self-corrugated surfaces

This article has been downloaded from IOPscience. Please scroll down to see the full text article.

2012 Nanotechnology 23 495712

(<http://iopscience.iop.org/0957-4484/23/49/495712>)

View [the table of contents for this issue](#), or go to the [journal homepage](#) for more

Download details:

IP Address: 147.46.56.173

The article was downloaded on 19/11/2012 at 12:30

Please note that [terms and conditions apply](#).

Electrical and structural properties of antimony-doped p-type ZnO nanorods with self-corrugated surfaces

Jang-Won Kang¹, Yong-Seok Choi¹, Minhyeok Choe¹, Na-Yeong Kim², Takhee Lee³, Bong-Joong Kim¹, C W Tu² and Seong-Ju Park^{1,2}

¹ School of Materials Science and Engineering, Gwangju Institute of Science and Technology, Gwangju 500-712, Korea

² Department of Nanobio Materials and Electronics, Gwangju Institute of Science and Technology, Gwangju 500-712, Korea

³ Department of Physics and Astronomy, Seoul National University, Seoul 151-744, Korea

E-mail: sjpark@gist.ac.kr

Received 22 August 2012, in final form 5 October 2012

Published 16 November 2012

Online at stacks.iop.org/Nano/23/495712

Abstract

We report on p-type conductivity in antimony (Sb)-doped ZnO (ZnO:Sb) nanorods which have self-corrugated surfaces. The p-ZnO:Sb/n-ZnO nanorod diode shows good rectification characteristics, confirming that a p–n homojunction is formed in the ZnO nanorod diode. The low-temperature photoluminescence (PL) spectra of the ZnO:Sb nanorods reveal that the p-type conductivity in p-ZnO:Sb is related to the $\text{Sb}_{\text{Zn}}-2\text{V}_{\text{Zn}}$ complex acceptors. Transmission electron microscopy (TEM) analysis of the ZnO:Sb nanorods also shows that the p-type conductivity is attributed to the $\text{Sb}_{\text{Zn}}-2\text{V}_{\text{Zn}}$ complex acceptors which can be easily formed near the self-corrugated surface regions of ZnO:Sb nanorods. These results suggest that the $\text{Sb}_{\text{Zn}}-2\text{V}_{\text{Zn}}$ complex acceptors are mainly responsible for the p-type conductivity in ZnO:Sb nanorods which have corrugated surfaces.

(Some figures may appear in colour only in the online journal)

1. Introduction

ZnO has been extensively investigated for applications in electronic and optoelectronic devices such as field-effect transistors, laser diodes, light-emitting diodes (LEDs) and photo detectors because it has a wide direct band gap (3.37 eV), a high saturation velocity ($3.2 \times 10^7 \text{ cm s}^{-1}$) and a large exciton binding energy (60 meV) [1–5]. However, the main obstacle to the application of ZnO in electronic and optoelectronic devices is the difficulty in obtaining p-type ZnO, because p-type conductivity and its origins are still not well understood in ZnO. In the effort to achieve p-type doping of ZnO, much attention has been paid to the large size group V elements including phosphorus (P), arsenic (As) and antimony (Sb) [6–12]. Because the large size dopants do not directly substitute the oxygen elements in ZnO because of the large

differences in their ionic radii (1.38 Å for O, 2.12 Å for P, 2.22 Å for As and 2.45 Å for Sb) [13], it is expected that the vacancies near extended defects such as stacking faults and dislocations in ZnO films will play an important role in accommodating the large size dopants in ZnO films. It is therefore necessary to understand the effects of structural defects and vacancies on the p-type conductivity of ZnO when doped with a large size dopant, such as Sb.

Recently, Park *et al* have reported on heterojunction LEDs composed of p-type Sb-doped ZnO (ZnO:Sb), InGaN/GaN multiple quantum wells and n-GaN [14]. They reported that p-type conductivity was observed in columnar ZnO:Sb films which have self-corrugated surfaces. The authors investigated the electrical, optical and structural properties of a ZnO:Sb nanorod (NR) that had been separated from the NR ZnO film to understand the reasons why

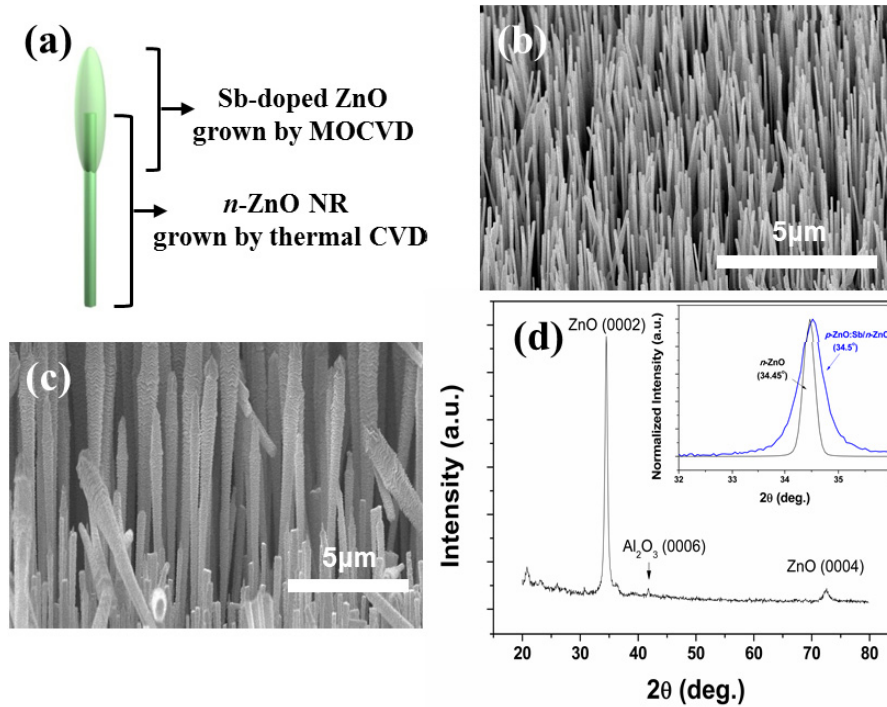


Figure 1. (a) Schematic of a ZnO:Sb/ZnO NR. (b) SEM image of ZnO NRs grown by CVD. (c) SEM image of ZnO:Sb/ZnO NR arrays. (d) XRD θ - 2θ spectra of n-ZnO and p-ZnO:Sb/n-ZnO NRs. The inset shows the magnified (0002) diffraction peaks of the n-ZnO and p-ZnO:Sb/n-ZnO NRs.

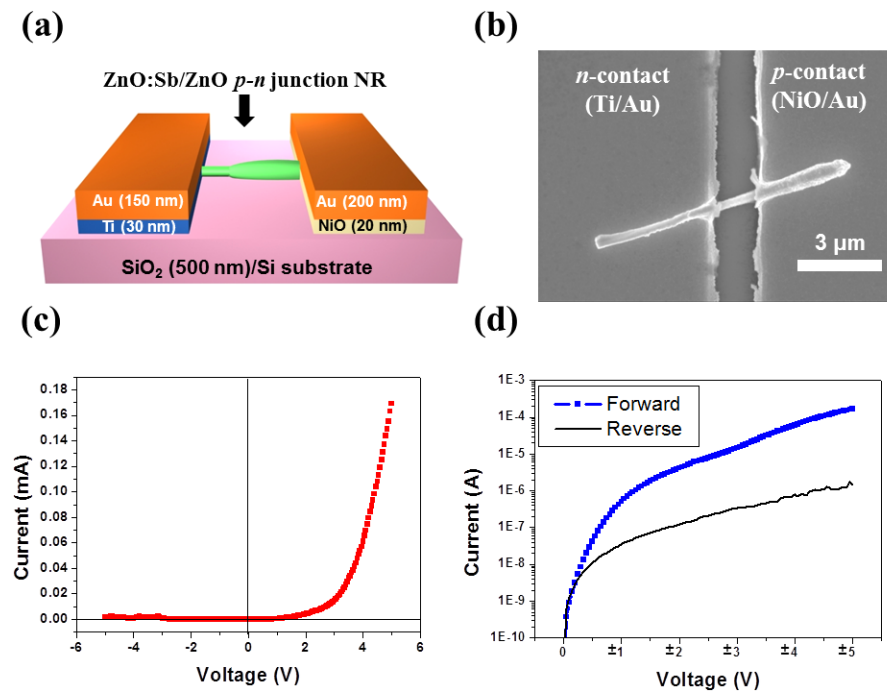


Figure 2. (a) Schematic of the ZnO:Sb/ZnO diode. (b) SEM image of the ZnO:Sb/ZnO diode. (c) I - V characteristics of the ZnO:Sb/ZnO diode at room temperature. (d) Semilogarithmic plot of the I - V characteristics of the ZnO:Sb/ZnO diode under forward and reverse biases.

p-type conductivity can be readily observed in a columnar ZnO:Sb film which has a self-corrugated surface. In this paper, we report on the p-type properties and the plausible origin of p-type conductivity of ZnO:Sb NRs with corrugated surfaces.

2. Experimental details

An NR ZnO diode composed of n-ZnO and p-ZnO:Sb NRs was fabricated to investigate the electrical properties of the p-ZnO:Sb NRs. The n-ZnO NRs were first grown

on a *c*-plane sapphire substrate by thermal chemical vapor deposition (CVD) [15]. After a 3 nm-thick Au catalyst layer had been deposited on the sapphire substrate by electron-beam (e-beam) evaporation, the Au-coated substrate and a 1:1 mixture of ZnO and graphite powder in an alumina boat were transferred to a quartz tube inside a horizontal furnace. The ZnO and graphite powder mixture was reacted at 950 °C for 30 min. A gas mixture of oxygen (2 sccm) and argon (100 sccm) was then flowed into the CVD chamber, and the chamber pressure was increased to 20 Torr. After the growth of n-ZnO NRs, the sample was transferred to a ZnO metalorganic chemical vapor deposition (MOCVD) reactor to grow the p-type ZnO NRs on top of the n-ZnO NRs. Diethylzinc, trimethylantimony and O₂ gas (99.999% purity) were used as the sources for Zn, Sb and oxygen, respectively. After the growth of the ZnO:Sb layer on the n-ZnO NRs, the samples were then annealed at 700 °C for 1 min in a nitrogen environment to activate the Sb dopant. A p-ZnO:Sb/n-ZnO homojunction NR diode was then fabricated by using NiO (20 nm)/Au (200 nm) and Ti (30 nm)/Au (100 nm) as the p- and n-Ohmic electrodes, respectively. The NiO/Au film was used to form an Ohmic contact to the p-ZnO [4, 16, 17]. The optical and structural properties of the p-ZnO:Sb/n-ZnO homojunction NR diodes were investigated by low-temperature photoluminescence (PL) and transmission electron (TEM) measurements.

3. Results and discussion

Figure 1(a) shows a schematic of the ZnO:Sb/ZnO homojunction NR. The ZnO:Sb NR was grown by MOCVD and the n-ZnO NR was grown by thermal CVD. As shown in the scanning electron microscope (SEM) image in figure 1(b), vertically aligned ZnO NRs were grown by thermal CVD. The SEM image in figure 1(c) shows that the ZnO:Sb NRs were grown on top of the ZnO NRs, forming ZnO:Sb/ZnO homojunction NRs that had corrugated surfaces, particularly in the Sb-doped region, as illustrated in figure 1(a). Figure 1(d) shows the XRD θ - 2θ spectra of n-ZnO and p-ZnO:Sb/n-ZnO NRs after post-annealing. The XRD pattern of the p-ZnO:Sb/n-ZnO NR was not significantly changed except for the slight shift in the peak position and broadening of ZnO(0002) peak, as shown in the inset of figure 1(d), compared to undoped n-ZnO. This result indicates that Sb is effectively doped into ZnO and ZnO:Sb is a single crystalline structure without any phase separation.

To measure the electrical properties of the p-n homojunction ZnO:Sb/ZnO NR, a p-ZnO:Sb/n-ZnO NR diode was fabricated by performing a rapid thermal annealing (RTA) to activate the Sb dopant in the ZnO. Figures 2(a) and (b) show a schematic diagram and a SEM image of the ZnO:Sb/ZnO NR diode. The I - V characteristics of the p-ZnO:Sb/n-ZnO NR diode are shown in figure 2(c). The NR ZnO diode shows good rectifying I - V characteristics, with a turn-on voltage of 3.3 V, which is in good agreement with the expected value for a ZnO diode with a band gap energy of 3.37 eV at room temperature. The rectification ratio of forward to reverse bias current is 105:1 at a bias

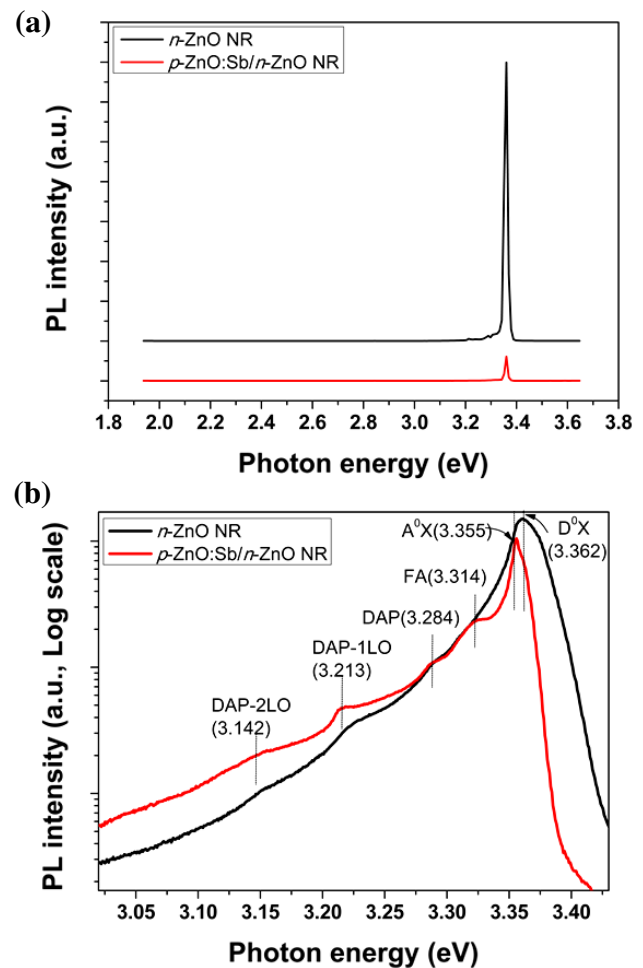


Figure 3. (a) Low-temperature PL (10 K) spectra of p-ZnO:Sb/n-ZnO NRs. (b) Near-band-edge emission spectra of p-ZnO:Sb/n-ZnO NRs.

voltage of ± 5 V, as shown in figure 2(d). The ideality factor for the ZnO:Sb/ZnO NR diode was estimated to be 2.8 for low voltages ($0 \text{ V} \leq V \leq 1 \text{ V}$) and 18 for higher voltages ($> 1 \text{ V}$). These rectifying characteristics of the ZnO:Sb/ZnO p-n homojunction NR diode are similar to those of p-n ZnO homojunction diodes which were formed with high quality p-type ZnO films [18, 19], showing that the ZnO:Sb NRs with corrugated surfaces have p-type conductivity after a thermal activation process.

The PL spectra of the n-ZnO NRs and the p-ZnO:Sb NRs were measured at a low temperature of 10 K, as shown in figure 3. Defect-related deep-level emission was not observed on these PL spectra. Figure 3(a) shows that the intensity of the main PL peak of the p-ZnO:Sb NRs is much lower than that of the n-ZnO NRs. The decrease in PL peak intensity is attributed to the degradation of the structural quality of p-ZnO:Sb NRs caused by the Sb doping of ZnO. The intense near-band-edge (NBE) emission at 3.362 eV, as shown in figure 3(b), corresponds to neutral-donor-bound excitons (D^0X). The emission lines at 3.355 and 3.314 eV are related to an acceptor-bound exciton (A^0X) transition and a free-electron to neutral-acceptor (FA) transition, respectively [20–22]. The emission line at 3.284 eV originates from donor-acceptor

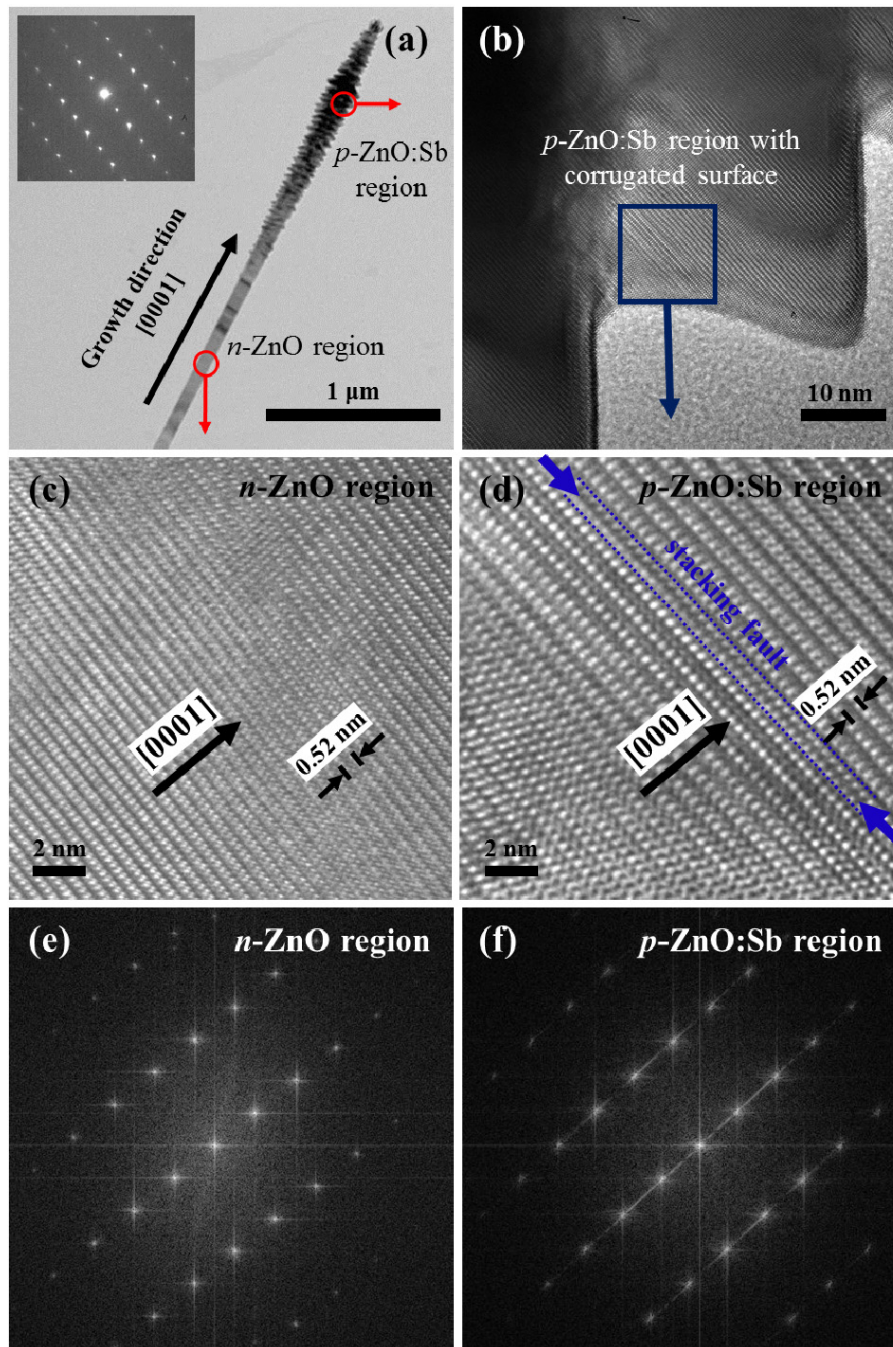


Figure 4. (a) TEM image of a p-ZnO:Sb/n-ZnO NR. The inset shows the SAED pattern of the NRs. (b) TEM image of the ZnO:Sb region in the p-ZnO:Sb/n-ZnO NR. (c) High-resolution TEM image of the n-ZnO region in the p-ZnO:Sb/n-ZnO NR. (d) Magnified high-resolution TEM image of the p-ZnO:Sb region; a stacking fault is marked with an arrow. (e, f) FFT images of (e) n-ZnO and (f) p-ZnO regions.

pair (DAP) transitions. The emission lines at 3.213 eV and 3.142 eV are related to the longitudinal optical (LO) phonon replicas of the DAP, which have energy separations of 71 meV. Based on these PL results, the binding energy of an acceptor (E_A) can be obtained from the following equation [9]:

$$E_A = E_g - E_{FA} + kT/2, \quad (1)$$

where E_g is the band gap of ZnO at 10 K ($E_g = 3.437$), and E_{FA} is the FA energy peak position at 10 K. The binding energy of the acceptors is estimated to be 124 meV and this value for the p-ZnO:Sb NR is very close to the

previously reported values of 124–137 meV [12, 20–22]. It has been reported that the large-mismatched group V dopants do not substitute for the O sites but rather for the Zn sites, each forming an $A_{Zn}-2V_{Zn}$ ($A = P, As, Sb$) complex with two spontaneously induced Zn vacancies [9]. These binding energies were reported to be indicative of the formation of $Sb_{Zn}-2V_{Zn}$ complex acceptors in p-type ZnO material [9, 12], suggesting that complex-type acceptors are formed in p-ZnO:Sb NRs with corrugated surfaces.

The microstructures of the p-ZnO:Sb and n-ZnO regions of an NR ZnO diode were analyzed by TEM. Figures 4(a)

and (b) show that the corrugated surface is formed only in the p-ZnO:Sb region of the NR ZnO diode. As shown in figures 4(c) and (d), the p-ZnO:Sb/n-ZnO NR diode is highly *c*-axis oriented in both the p-ZnO:Sb and n-ZnO regions, indicating that the p-ZnO:Sb NR is epitaxially grown on the n-ZnO NR. The selective area electron diffraction (SAED) pattern in the inset of figure 4(a) shows that the p-ZnO:Sb/n-ZnO NR has a single crystalline nature, which is in good agreement with the fast Fourier transform (FFT) images in figures 4(e) and (f). The high-resolution (HR) TEM and FFT images of the n-ZnO region show that the n-ZnO NR does not include any visible defects, as shown in figure 4(c) and in the FFT image of the n-ZnO region in figure 4(e). However, the p-ZnO:Sb NR contains stacking faults, as indicated by an arrow in figure 4(d). The streaks in the FFT image of figure 4(f) indicate that a number of stacking faults exist in the p-ZnO:Sb region. It has been reported that $Sb_{Zn}-2V_{Zn}$ complex acceptors, which can lead to p-type conductivity in ZnO, can be formed more easily by combining Sb_{Zn} with Zn vacancies formed near stacking faults and dislocations [23]. In this study, the PL and TEM analyses of the p-ZnO:Sb/n-ZnO NR diodes indicate that the p-type conductivity of the p-ZnO:Sb NR is closely related to the $Sb_{Zn}-2V_{Zn}$ complex acceptors that are formed near the corrugated surface regions of p-ZnO:Sb NRs. Therefore, it is believed that the p-type conductivity which is readily observed in columnar p-ZnO:Sb films and p-ZnO:Sb NRs which have self-corrugated surfaces is caused by $Sb_{Zn}-2V_{Zn}$ complex-type acceptors.

4. Conclusions

To understand the p-type conductivity in columnar ZnO:Sb structures which have self-corrugated surfaces, p-ZnO:Sb NRs with self-corrugated surfaces were grown on top of an n-ZnO NR template. A single p-ZnO:Sb/n-ZnO NR diode shows good diode characteristics, confirming that p-n homojunctions are formed in the ZnO NR diodes. Low-temperature PL and TEM studies show that the origin of p-type conductivity in p-ZnO:Sb NRs with self-corrugated surfaces is closely related to the $Sb_{Zn}-2V_{Zn}$ complex-type acceptors formed near stacking faults in the corrugated surface region of the p-ZnO:Sb.

Acknowledgments

This work was supported by the World Class University (WCU) program through a grant provided by the Ministry

of Education, Science and Technology (MEST) of Korea (Project No. R31-2008-000-10026-0) and by the Inter-ER Cooperation Projects (Grant No. R0000499) of the Ministry of Knowledge Economy of Korea.

References

- [1] Choi Y S, Kang J W, Hwang D K and Park S J 2010 *IEEE Trans. Electron Devices* **57** 26–41
- [2] Cha S N, Jang J E, Choi Y, Amaratunga G A J, Ho G W, Welland M E, Hasko D G, Kang D -J and Kim J M 2006 *Appl. Phys. Lett.* **89** 263102
- [3] Tang Z K, Wong G K L, Yu P, Kawasaki M, Ohtomo A, Koinuma H and Segawa Y 1998 *Appl. Phys. Lett.* **72** 3270–2
- [4] Lim J H, Kang C K, Kim K K, Park I K, Hwang D K and Park S J 2006 *Adv. Mater.* **18** 2720–4
- [5] Huang J, Wang L, Xu R, Tang K, Shi W and Xia Y 2009 *Semicond. Sci. Technol.* **24** 075025
- [6] Hwang D K, Oh M S, Choi Y S and Park S J 2008 *Appl. Phys. Lett.* **92** 161109
- [7] Ryu Y R, Zhu S, Look D C, Wrobel J M, Jeong H M and White H W 2000 *J. Cryst. Growth* **216** 330–4
- [8] Xiu F X, Mandalapu L J, Zhao D T, Liu J L and Beyermann W P 2005 *Appl. Phys. Lett.* **87** 152101
- [9] Limpijumngong S, Zhang S B, Wei S H and Park C H 2004 *Phys. Rev. Lett.* **92** 155504
- [10] Xiu F X, Yang Z, Mandalapu L J, Liu J L and Beyermann W P 2006 *Appl. Phys. Lett.* **88** 052106
- [11] Ryu Y R, Lee T S and White H W 2003 *Appl. Phys. Lett.* **83** 87–9
- [12] Xiu F X, Yang Z, Mandalapu L J, Zhao D T and Liu J L 2005 *Appl. Phys. Lett.* **87** 252102
- [13] Avrutin V, Silversmith D J and MoRkoc D 2010 *Proc. IEEE* **98** 1269–80
- [14] Park T Y, Choi Y S, Kim S M, Jung G Y, Park S J, Kwon B J and Cho Y H 2011 *Appl. Phys. Lett.* **98** 251111
- [15] Yang P, Yan H, Mao S, Russo R, Johnson J, Saykally R, Morris N, Pham J, He R and Choi H J 2002 *Adv. Funct. Mater.* **12** 323–31
- [16] Kong J, Chu S, Olmedo M, Li L, Yang Z and Liu J L 2008 *Appl. Phys. Lett.* **93** 132113
- [17] Chu S, Lim J H, Mandalaph L J, Yang Z, Li L and Liu J L 2008 *Appl. Phys. Lett.* **92** 152103
- [18] Ryu Y R, Lee T S, Leem J H and White H W 2003 *Appl. Phys. Lett.* **83** 4032
- [19] Lu J G, Ye Z Z, Yuan G D, Zeng Y J, Zhuge F, Zhu L P, Zhao B H and Zhang S B 2006 *Appl. Phys. Lett.* **89** 053501
- [20] Zhao J Z, Liang H W, Sun J C, Feng Q J, Bian J M, Zhao Z W, Zhang H Q, Hu L Z and Du G T 2008 *Electrochem. Solid State Lett.* **11** H323–6
- [21] Zang C H, Zhao D X, Tang Y, Guo Z, Zhang J Y, Shen D Z and Liu Y C 2005 *Chem. Phys. Lett.* **452** 148–51
- [22] Przewdzicka E, Kaminska E, Pasternak I, Piotrowska A and Kossut J 2007 *Phys. Rev. B* **76** 193303
- [23] Guo W, Allenic A, Chen Y B, Pan X Q, Che Y, Hu Z D and Liu B 2007 *Appl. Phys. Lett.* **90** 242108